Atomic simulations of the dynamic properties of the 30° partial dislocation in Si crystal

Chao-ying Wang,* Qing-yuan Meng, Kang-you Zhong, and Zhi-fu Yang
Department of Astronautical Science and Mechanics, Harbin Institute of Technology, Harbin, 150001, People's Republic of China
(Received 18 December 2007; revised manuscript received 2 March 2008; published 29 May 2008)

The dynamic properties of the 30° partial dislocation in Si have been investigated by the molecular dynamics (MD) and nudged elastic band (NEB) methods. The migration processes are involved with the five different defects: left kink (LK), right kink (RK), reconstruction defect (RD), LK-RD complex (LC) and RK-RD complex (RC). According to the recorded migration steps, it is found that the motions of kinks are carried out by the transformation between kinks and their intermediate states under a majority of conditions. However, for the LK, one or more kink pairs are produced during its motion under relatively higher temperature and shear stress conditions. Moreover, RK dissociates to the RD+RC structure under the similar conditions. The velocity curves of LK and RK indicate that the above phenomena can promote the motion of the 30° partial dislocation. All of these MD results are in good agreement with the migration barriers, which are computed by the NEB method. Both MD results and migration energies indicate that the migration properties of the 30° partial dislocation are involved with the core structure of kinks. In addition, the RD can lower the migration energies of LK and RK. Thus, the LC and RC, especially the RC, can greatly enhance the mobility of the 30° partial dislocation in comparison with LK and RK.

DOI: 10.1103/PhysRevB.77.205209 PACS number(s): 61.72.Lk, 61.72.Qq, 71.15.Pd

I. INTRODUCTION

Dislocations in cubic diamond lattice materials (Si, Ge) are of practical and fundamental importance in modern semiconductor techniques. They are not only related to the plastic deformation behavior but also concerned with the electronic and optical properties of micro-electro devices. In the earlier studies, the microscopic dislocation structures in Si have been studied in the atomic scale.[1–3] Recently, the research interest has been concentrated on the dynamic properties of the dislocations.[4–9]

The primary mobile dislocations in Si are the 60° dislocation[10] and screw dislocation, which orientate along ⟨110⟩ and glide in the {111} plane.[11] The 60° dislocation is known to dissociate into 30° and 90° partial dislocations, bounding a ribbon of intrinsic stacking fault (ISF).[12] The screw dislocation can also dissociate into two 30° partial dislocations, which are separated by the ISF too.[13] Moreover, both of the above dislocation dissociations have been proved energetically favorable.[3] For these two type of partial dislocations, there is a consensus that the 30° partial dislocation predominates the dislocation mobility. Thus, the 30° partial dislocation is chosen to explore the dynamic properties in this work.

The motion of the 30° partial dislocation occurs by nucleation and migration of kinks along the dislocation line in Si.[14,15] In the reconstructed 30° partial dislocation, kinks and reconstruction defects[16] (RDs) can be considered as the fundamental type of defects, which are illustrated in Fig. 1. This RD can be identified by a dangling bond, which is also referred to as an antiphase defect (APD).[17] In the previous researches, it was mainly concerned with the pure kinks: left kink (LK) and right kink (RK).[18–20] However, for the kink-RD complexes, i.e., the LK-RD complex (LC) and RK-RD complex (RC), which are formed by the bonding of RD with LK and RK, respectively,[21] were not taken into account. In fact, all of the intrinsic defects: LK, RK, LC, RC, and RD should be considered in the 30° partial dislocation motion. These five types of defects and their interatomic interactions make the dynamic migration processes more complex. So it is necessary to investigate the dynamic properties of the 30° partial dislocation more thoroughly and completely.

The fundamental theory of the atomic simulations of the 30° partial dislocation motion is based on the activation energy Q, which is composed of the kink formation energy F_k and migration barrier W_m.[18,20–22] Although many precise methods such as the tight-binding (TB)[23] and *ab initio* methods have been applied, very little is known about the underlying dynamic details. In other words, a detailed atomic scale understanding of the complex migration processes are not available up to now. The purpose of this research is to reveal the dynamic properties of the 30° partial dislocation in Si. By performing a series of molecular dynamics (MD) simulations over a range of temperature and shear stress, a particular description of the mobile processes of kinks with functions of interatomic interactions is given. Furthermore, the nudged elastic band (NEB) method[24] is employed to calculate the kink migration barriers W_m, which are used for verifying the MD simulation results.

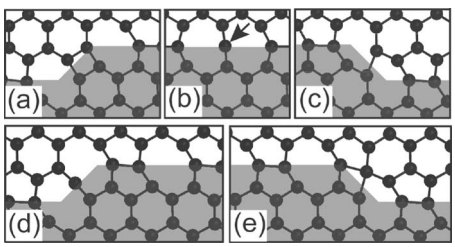

FIG. 1. Five types of defects at the 30° partial dislocation in the {111} plane. (a) Left kink (LK). (b) Reconstruction defect (RD). (c) Right kink (RK). (d) LK-RD complex (LC). (e) RK-RD complex (RC). The shaded areas indicate the intrinsic stacking fault (ISF).

II. MD SIMULATION AND RESULTS

A. MD simulation procedure

In this work, the MD method, together with the environment-dependent interatomic potential[25] (EDIP), is employed to conduct the atomistic dynamic calculations. To accomplish a real physical process, it usually requires tens of thousands of atoms in the MD simulations. However, such simulation can not be easily accomplished by the *ab initio* and TB methods. In this case, the empirical potentials were chosen to deal with these dislocation models. Although there are lots of empirical potentials, which have been developed to deal with different systems, only the EDIP model can be properly used for describing both the 30° and 90° partial dislocations in Si.[26] The interaction model of EDIP contains two-body and three-body terms, which depend on the local atomic environment through an effective coordination number.[25] In addition, its functional expression contains the essential features of chemical bonding in the bulk, which can give good performances of describing interatomic forces in Si bulk phase and defects.[25]

The MD simulations were carried out under the NPT ensemble, which means that the particle number N, pressure P, and temperature T are kept constant. In the integral of the Newtonian equations of motion, the Verlet algorithm[27] is used and the time step is 1 fs. In this work, the shear stress is applied by means of the Parrinello–Rahman[28] method along the Burgers vector of the 30° partial dislocation. In order to use the periodic boundary conditions (PBC) in three directions of the MD model, a dislocation dipole with opposite Burger vectors is introduced. The shortcoming of this method is that we should consider the interaction between the two dislocations in one dislocation dipole and the interaction between the dislocation dipole and its images. However, due to the sufficient model sizes and large shear stress (1–2 GPa) specified in the following, these interactions can be neglected without significant influence on the final results.

For LK and RC, the corresponding MD model vectors are $4[111]$, $20[11\bar{2}]$, and $11.5[1\bar{1}0]$, containing 11 040 atoms. For RK and LC, the corresponding MD model vectors are $4[111]$, $20[11\bar{2}]$, and $10.5[1\bar{1}0]$, containing 10 080 atoms. In each model, two kinks are placed in the {111} plane, which are separated from each other by a distance of $10[11\bar{2}]$.

A series of MD simulations were conducted for each of the four kink species. In this work, a constant shear stress with four different values (1, 1.5, 2, and 2.5 GPa) is applied to each model first, and then the constant temperature is chosen from 850 K to 2500 K at a step interval of 50 K. For each case of calculations, the total time duration is 300 ps, and the configurations of kinks are recorded at a time step of 0.1 ps. Finally, a series of detailed dynamic processes were obtained for the four kink species LK, RK, LC, and RC eventually.

B. MD simulation results

The migration processes of the LK and RK under low temperature or shear stress conditions are shown in Figs. 2(a)–2(c) and Figs. 2(d)–2(f), respectively. The reconstructed

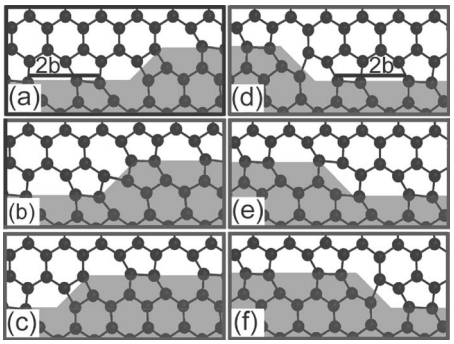

FIG. 2. Pure kink migration processes in the {111} plane under the low temperature or shear stress conditions. The migration path of LK in one repeated distance 2b: (a) LK, (b) LK1, which is the intermediate state of LK, (c) LK′. The migration path of RK: (d) RK, (e) RK1, which is the intermediate state of RK, (f) RK′. The shaded areas indicate the ISF.

core structure of the 30° partial dislocation has a repeated distance of 2b (b is the Burgers vector length of $(1/2)\langle 110\rangle$). In one migration period of 2b, the migration starts from LK (RK). When the kink moves by half of the period, LK (RK) transforms into the intermediate state LK1 (RK1). In the following half-repeated distance, LK1 (RK1) transforms into LK′ (RK′), which has the same kink structure as LK (RK). It is known from Fig. 2 that transformations of the above processes are carried out by the bond breaking, bond rotation, and bond exchange. Moreover, it is important to note that the atom in the center of LK, RK, and their intermediate states is fourfold coordinated. Due to the saturated core atoms, the pure kinks and their translation states may remain relatively stable under the normal conditions. The above results can also be used to explain why similar migration processes have been observed by many other researchers.[18,20–22]

The migration processes of LC and RC in one migration period are shown in Figs. 3(a)–3(d) and Figs. 3(e)–3(h), respectively. Similar to LK and RK, the motion steps of LC

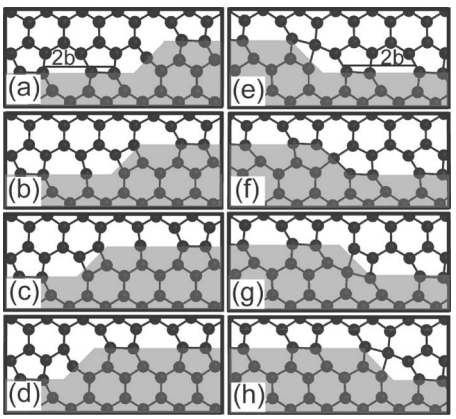

FIG. 3. Kink-RD complexes migration processes in the {111} plane. The migration path of LC in one repeated distance: (a) LC, (b) LC1, which is the first intermediate state, (c) LC2, which is the second intermediate state, (d) LC′. The migration path of RC: (e) RC, (f) RC1, which is the first intermediate state, (g) RC2, which is the second intermediate state, (h) RC′. The shaded areas indicate the ISF.

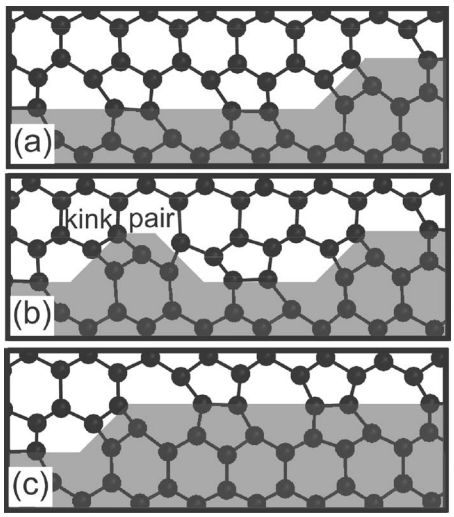

FIG. 4. LK (kink pair) migration processes in the {111} plane. (a) LK. (b) A kink pair produced. (c) LK′. The shaded areas indicate the ISF.

(RC) are LC (RC)→LC1 (RC1)→LC2 (RC2)→LC′ (RC′), where LC1 (RC1) and LC2 (RC2) are the sequent intermediate states. It can be seen from Fig. 3 that the motion are conducted by the bond breaking and bond distortion. Besides, the center atom of LC and its intermediate states is threefold coordinated. Instead of the unsaturated bond of LC, there is supersaturated atom, which is fivefold coordinated in the center of RC and its intermediate states. These unsaturated and supersaturated bonds make the kink-RD complexes possess different dynamic characteristics compared with the pure kinks with saturated bonds.

Under the relatively higher temperature and shear stress conditions, the LK and RK exhibit absolutely different dynamic properties. For the LK, it produces one or more kink pairs, which are composed of LK and RK. When RK (LK) encounters another LK (RK), they annihilate each other. These migration mechanisms shown in Fig. 4 are consistent with Hirth and Lothe's theory.[14] To distinguish the migrations, which are shown in Figs. 2(a)–2(c), the motion shown in Fig. 4 can be taken as migration processes of LK (kink pair). For the RK, the complex migration processes are shown in Fig. 5. When the external conditions approach comparatively higher values, the RK can dissociate into the RD+RC structure, which is shown in Fig. 5(b). This dissociation had been explored by Bulatov *et al.*, who also declared that this action is easier to take place than the action of LK→RD+LC.[21] After the dissociation, the motion of RK is carried out by the motion of RC in company with RD. To distinguish the migration processes, which are shown in Figs. 2(e) and 2(f), the motion processes shown in Fig. 5 can be considered as migration processes of RK (RD+RC).

As shown from Fig. 2 to Fig. 5, the dynamic properties of kinks are very complicated. Especially the LK and RK, they show various properties under different conditions. To further reveal the complex dynamics properties of the 30° partial dislocation, the velocities and migration categories of pure kinks over a range of temperature and shear stress are shown in Fig. 6. It is seen that the velocities are very small

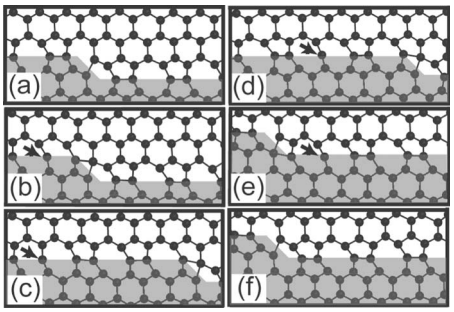

FIG. 5. RK (RC+RD) migration processes in the {111} plane under the relatively higher temperature and shear stress conditions. (a) RK. (b) RK→RD+RC. (c)–(e) The motion of RC in company with RD. (f) RK′. The arrows point to the RD and the shaded areas indicate the ISF.

and increase slowly under the low temperature or shear stress conditions. Although both LK and RK are less mobile at the beginning, RK moves obviously faster than the LK under the same conditions. When the temperature is higher than 1000 K under the shear stress of 2.5 GPa, the velocities of LK (kink pair) and RK (RD+RC) jump suddenly and increase significantly. The similar results occur for the RK (RD+RC) at 1150 K and 1200 K under the shear stress of 2 GPa. All of the above results show that the LK (kink pair) and RK (RC+RD) under relatively higher temperature and shear stress move faster than the LK and RK, which is due to the presence of other defects, i.e., kink pair, RC and RD. Thus, it can be concluded that kink pair and the RC+RD structure may make the 30° partial dislocation more mobile.

III. NEB CALCULATION AND RESULTS

In Si, the migration barriers not only predominate the dislocation velocity,[18,29] they also provide the relation between the atomistic structures and the mobility behaviors. Thus, the migration energies of the four kink species are necessary to be calculated in order to verify the dynamics results presented in Sec. II. To get the comparatively precise results, the NEB method joined with the semiempirical potential TB is used for the calculations.

The NEB method is efficient for finding the minimum energy path (MEP) between two states. To get the MEP of

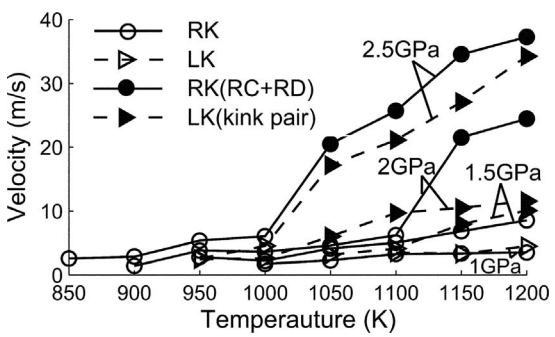

FIG. 6. The velocities as well as migration categories of LK and RK plotted over a range of temperature and shear stress.

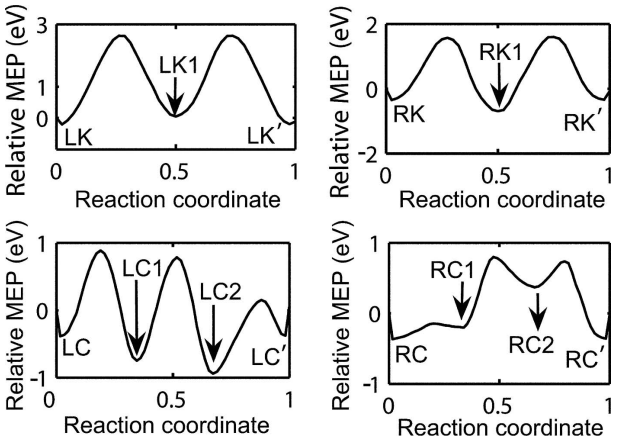

FIG. 7. The relative minimum energy paths (MEPs) in one repeated distance for the LK, RK, LC, and RC.

kinks in one repeated distance, we create 14 small size models, which correspond to the configurations shown in Figs. 2 and 3. Among these models, LK and RC contain 540 atoms, and RK and LC contain 612 atoms. By regarding each start state of kinks as the ground state in one repeated distance, the relative MEPs of the four kink species are plotted against the reaction coordinate in Fig. 7. In addition, the computed migration barriers of LK, RK, LC, and RC obtained by others[20–22] together with the present results, are shown in Table I.

It can be seen from Table I that all of the computational results do not deviate too far from experimental data, which are in the range of 1.2 (Ref. 12)–1.8 eV (Ref. 31). The results of this work are a bit higher than the data of experiment, Ref. 21 and Ref. 22. Nunes *et al.*[22] claimed their results were in good agreement with the experiment, but the computed kinks migration barriers of the 30° partial should be higher than the experimental results. This is due to the fact that the experimental data include both the 30° and 90° partial[30,31] since the 90° partial is more mobile than the 30° partial,[30,32] and the barrier energy should be lower than the 30° partial, correspondingly. Therefore, it can be concluded that the present results are reasonably acceptable.

TABLE I. The migration barrier W_m of LK, RK, LC, and RC calculated by the use of different potentials: Stillinger–Weber (SW), total-energy tight-binding (TBTE), density-functional-based tight-binding (DFTB), and tight-binding (TB).

	W_m (eV)			
Author (potential)	LK	RK	LC	RC
Bulatov *et al.* (SW)[a]	0.82	0.74	0.22	1.04
Nunes *et al.* (TBTE)[b]	1.52	2.03	0.49	0.8
Blumenau *et al.* (DFTB)[c]	3.5	2.7		
This work (TB)	2.84	2.29	1.82	1.12

[a]Reference 21.
[b]Reference 22.
[c]Reference 20.

IV. DISCUSSION

Actually, all of the migrations of kinks are carried out by the bond breaking, bending, and stretching. In consideration of the core structures, which are different for each type of kinks, the associated migration abilities are different, too. For the LK and RK, the center atoms are fourfold coordinated and the migration barriers are 2.84 and 2.29 eV, respectively. The migration barriers of LC and RC are 1.82 and 1.12 eV, which have threefold and fivefold coordinate atom in the center of kinks, correspondingly. It is distinct that the migration barriers of pure kinks, which have saturated bonds, are higher than the kink-RD complexes, which have unsaturated or supersaturated bonds. It is shown that RD can lower the migration energies of pure kinks. Moreover, LC and RC are more mobile than the LK and RK. In summary, it can be concluded that the migration abilities of kinks are determined by the core structures of kinks.

It is known from Fig. 6 and Table I that the kinks velocity properties are in good agreement with the migration barriers. First, the migration barrier of LK is higher than RK, which leads to a physical picture in Fig. 6 that RK move relatively faster than LK under the same conditions. In the other side, both barriers are very high, which result in very low velocities for pure kinks. Among the four different species of kinks, RC has the lowest barrier of 1.12 eV. Thus, the presence of RC during the motion of RK (RC+RD) makes the velocity jump and increase significantly under the shear stress of 2.5 GPa and 2 GPa.

V. CONCLUSION

First, the dynamic properties of the 30° partial dislocation in Si were investigated by the MD method. By performing a series of MD simulations under different temperature and shear stress conditions, the migration processes of four kink species are recorded. It is found that under relatively lower temperature or shear stress conditions, the motion of LK and RK are carried out by the transformation between the pure kinks and their intermediate states. The LC and RC have the similar processes as the pure kinks, which have two intermediate states for each kink. Under relatively higher temperature and shear stress conditions, one or more kink pairs are produced during the migration processes of LK. Instead of the kink pair, RK dissociates into RD+RC structure during its motion. The velocity curves of LK and RK indicate that both kink pair and RC+RD may make the 30° partial dislocation move faster.

Second, the migration barriers of the four kink species are calculated by the NEB method, which is based on the TB potential. The migration energies indicate that the different motion abilities of these four kink species are in good agreement with the MD results. Both MD results and migration barriers show that the migration properties of the 30° partial dislocation are involved with the core structures of the four different species of kinks. RD may lower the migration energies of the pure kink by means of transformation of the kink center atom from saturated bond to unsaturated or supersaturated bond. For this reason, LC and RC are more active than LK and RK, which may make the 30° partial

dislocation more mobile. Moreover, it can be conclude that the RC has the largest contribution for facilitating the 30° partial dislocation movement because it has the lowest migration barrier compared with other kinks.

ACKNOWLEDGMENT

This work was supported by the NSF of China under Grant No. 10772062.

*chaoyingwang@gmail.com

[1] J. R. K. Bigger, D. A. McInnes, A. P. Sutton, M. C. Payne, I. Stich, R. D. King-Smith, D. M. Bird, and L. J. Clarke, Phys. Rev. Lett. **69**, 2224 (1992).
[2] M. S. Duesbery, B. Joos, and D. J. Michel, Phys. Rev. B **43**, 5143 (1991).
[3] A. T. Blumenau, M. I. Heggie, C. J. Fall, R. Jones, and T. Frauenheim, Phys. Rev. B **65**, 205205 (2002).
[4] H. Koizumi and T. Suzuki, Mater. Sci. Eng., A **400-401**, 76 (2005).
[5] B. Ya. Farber, Yu. L. Iunin, V. I. Nikitenko, V. I. Orlov, H. Alexander, H. Gottschalk, and P. Specht, Phys. Status Solidi A **138**, 557 (1993).
[6] I. Yonenaga and Koji Sumino, Appl. Phys. Lett. **69**, 1264 (1996).
[7] S. S. Quek, Y. Xiang, Y. W. Zhang, D. J. Srolovitz, and C. Lu, Acta Mater. **54**, 2371 (2006).
[8] G. Vanderschaeve and D. Caillard, Mater. Sci. Eng., A **462**, 418 (2007).
[9] A. Marzegalli, F. Montalenti, and L. Miglio, J. Phys.: Condens. Matter **17**, 7505 (2005).
[10] Y. B. Bolkhovityanov, A. K. Gutakovskii, V. I. Mashanov, O. P. Pchelyakov, M. A. Revenko, and L. V. Sokolov, J. Appl. Phys. **91**, 4710 (2002).
[11] M. S. Duesbery and G. Y. Richardson, Crit. Rev. Solid State Mater. Sci. **17**, 1 (1991).
[12] P. B. Hirsch, Mat. Sci. Technol. **1**, 666 (1985).
[13] P. E. Batson, Phys. Rev. Lett. **83**, 4409 (1999).
[14] J. P. Hirth and J. Lothe, *Theory of Dislocations*, 2nd ed. (Wiley, New York, 1982).
[15] H. Gottschalk, N. Hiller, S. Sauerland, P. Specht, and H. Alexander, Phys. Status Solidi A **138**, 547 (1993).
[16] V. V. Bulatov, J. F. Justoz, Wei Cai, Sidney Yip, A. S. Argon, T. Lenosky, M. de Koning, and T. Diaz de la Rubia, Philos. Mag. A **81**, 1257 (2001).
[17] P. B. Hirsch, J. Phys. (Paris), Colloq. **40**, C6-117 (1979).
[18] Norihisa Oyama and Takahisa Ohno, Phys. Rev. Lett. **93**, 195502 (2004).
[19] Y. M. Huang, J. C. H. Spence, and O. F. Sankey, Phys. Rev. Lett. **74**, 3392 (1995).
[20] A. T. Blumenau, R. Jones, T. Frauenheim, B. Willems, O. I. Lebedev, G. Van Tendeloo, D. Fisher, and P. M. Martineau, Phys. Rev. B **68**, 014115 (2003).
[21] V. V. Bulatov, S. Yip, and A. S. Argon, Philos. Mag. A **72**, 453 (1995).
[22] R. W. Nunes, J. Bennetto, and David Vanderbilt, Phys. Rev. B **57**, 10388 (1998).
[23] T. J. Lenosky, J. D. Kress, I. Kwon, A. F. Voter, B. Edwards, D. F. Richards, S. Yang, and J. B. Adams, Phys. Rev. B **55**, 1528 (1997).
[24] G. Mills and H. Jonsson, Phys. Rev. Lett. **72**, 1124 (1994).
[25] Martin Z. Bazant, Efthimios Kaxiras, and J. F. Justo, Phys. Rev. B **56**, 8542 (1997).
[26] J. F. Justo, Martin Z. Bazant, Efthimios Kaxiras, V. V. Bulatov, and Sidney Yip, Phys. Rev. B **58**, 2539 (1998).
[27] M. P. Allen and D. J. Tildesley, *Computer Simulation of Liquids* (Clarendon, Oxford, 1987).
[28] M. Parrinello and A. Rahman, J. Appl. Phys. **52**, 7182 (1981).
[29] H. R. Kolar, J. C. H. Spence, and H. Alexander, Phys. Rev. Lett. **77**, 4031 (1996).
[30] R. Hull, J. C. Bean, D. Bahnck, L. J. Peticolas, Jr., K. T. Short, and F. C. Unterwald, J. Appl. Phys. **70**, 2052 (1991).
[31] Y. Yamashita, K. Maeda, K. Fujita, N. Usami, K. Suzuki, S. Fukatsu, Y. Mera, and Y. Shitaki, Philos. Mag. Lett. **67**, 165 (1993).
[32] H. Gottschalk, N. Hiller, S. Sauerland, P. Specht, and H. Alexander, Phys. Status Solidi A **138**, 547 (1993).